Engineering and Technology Journal
Journal homepage: https://etj.uotechnology.edu.iq

Using Taguchi Design to Compare the Corrosion Behavior of Commercial Pure Ti Alloys Coated by Dip and Electrophoretic Deposition with YSZ

Marwan B. Hussein*, Ali M. Mustafa, Makarim H. Abdulkareem

Production Engineering and Metallurgy Dept., University of Technology-Iraq, Alsina'a street, 10066 Baghdad, Iraq.
*Corresponding author Email: pme.20.59@grad.uotechnology.edu.iq

HIGHLIGHTS

- Coatings that consist of YSZ nano-powder by dip coating on Cp-Ti and Ti-13Zr-13Nb were used.
- The coating exhibits good adhesion to the Cp-Ti and Ti-13Nb-13Zr alloy.
- The surface of the composite coatings was free from cracks.
- CP-Ti and Ti-13Zr-13Nb alloys have good corrosion resistance properties in Ringer's solution.

ARTICLE INFO

Handling editor: Omar Hassoon

Keywords:

Dip coating

Electrophoretic deposition

Corrosion

Taguchi

YSZ

ABSTRACT

This study makes experimental evaluations of the corrosion and tip tests of CP-Ti joint (commercial pure Ti) implant alloys coated with YSZ nanoceramic. A Taguchi design of experiments (DOE) strategy was used to create a thin adhesive covering utilizing dip coating and electrophoretic deposition techniques. An L9-type orthogonal Taguchi array determined how dip coating and electrophoretic deposition factors, such as temperature, voltage, YSZ concentration, time, and the degree of pulverizing the Ti alloy substrate, affected the deposition yield. The Ti alloys were coated using the optimal settings for the dip coating and electrophoretic deposition procedures as previously described, utilizing the output data from the thickness and adhesion experiments used to optimize the conditions of dip coating and electrophoretic deposition. The optimal conditions for electrophoretic deposition were 60 volts, 7 minutes, 15% concentration, and 400 grit of grinding. The optimal dip coating conditions were 60°C temperature, 10 seconds, 1% concentration, and 250 grit size of Grinding. High-resolution scanning electron microscopy (FE-SEM) images of the coated alloys were employed for the examination. The microstructure and thickness of the coated surfaces were further examined using optical microscopy and atomic force microscopy (AFM). The corrosion resistance of the best-coated Ti alloys was examined using electrochemical techniques such as polarizing (Tafel) and cyclic polarization in simulated bodily fluid (SBF). Using a tip tester, the coatings' adhesive strength was evaluated. The coated CP-Ti alloys were contrasted using the following corrosion-resistant values: Both coating alloys enhanced corrosion resistance in Ringer's solution at 37°C. However, the coated CP-Ti alloy by electrophoretic deposition corroded less quickly than the CP-Ti alloy by dip coating (3.031×10^{-3} vs 1.042×10^{-3} respectively).

1. Introduction

Due to its low density, outstanding corrosion resistance, and exceptional biocompatibility, Titanium (Ti) and its alloys are increasingly used in various disciplines, including orthodontics, dentistry, prosthodontics, and implantology. The user's material is too brief to be professionally redone. There is a link between a material's susceptibility to corrosion and its biocompatibility since the release of metal ions into their surrounding environment during corrosion might harm nearby tissues [1,2]. The user has specified a range of [3] numbers. To maximize the interfacial contact between the implant metal and surrounding tissues, surface modification research on metallic implants is essential. Bioactive substances are often used in the implants [4]. The coatings used on implants should have properties that encourage bone cell attachment and offer a variety of useful qualities, such as corrosion resistance, wear resistance, and antibacterial activity [5,6].

The surfaces of biomedical implants have been modified using various surface treatment methods, including the sol-gel approach, alkali and heat treatment, physical vapor deposition (PVD), and chemical vapor deposition (CVD). These approaches

http://doi.org/10.30684/etj.2023.143016.1557
Received 11 September 2023; Received in revised form 21 October 2023; Accepted 24 October 2023; Available online 06 December 2023
2412-0758/University of Technology-Iraq, Baghdad, Iraq

encourage cell adhesion and growth at the interface between the implants and surrounding tissues [7]. Several references have been given by the user among the various alloys examined.

Contrarily, electrophoretic deposition (EPD) has drawn a lot of attention because of its remarkable adaptability to a variety of materials, simple setup procedure, equipment cost effectiveness, few restrictions on substrate shape, and capacity to create intricate patterns and forms at low temperatures [8,9]. There are two separate steps in the EPD approach. Charged powder particles dispersed or suspended in either an aqueous or non-aqueous liquid are drawn to and subsequently stick to a conductive substrate with an opposing charge when exposed to a direct current (DC) electric field [10].

It could be important to execute a proper heat treatment after the coating application to improve the compactness of deposits and decrease the degree of porosity in EPD coatings. The use of titanium dioxide (TiO_2) for photovoltaic cells, hydroxyapatite in biomaterials, yttria-stabilized zirconia (YSZ) for solid oxide fuel cells, and YSZ for coatings, including thermal barriers are some current research advancements and specific application areas of electrophoretic deposition (EPD) coatings [11]. In biomedical applications, bioceramic coatings are frequently used to change the surface of implant materials, resulting in the formation of new surfaces with distinctive properties distinct from the underlying substrate. The dip coating technique is an alternative for applying coatings to orthopedic prosthetic systems. Compared to other coating techniques, the sol-gel process has many benefits, including increased flexibility and the capacity to control the coating's morphology, chemistry, and structural characteristics [12,13]. Additionally, it is possible to lower the sintering temperature by using the right additives [14]. Milella et al. [15] applied a bio-ceramic composite to a titanium substrate using the dip-coating method in their investigation. Due to its favorable thermal and mechanical qualities, partially yttria-stabilized zirconia in (8YSZ) has been used extensively as a thermal barrier coating (TBC) material. Low heat conductivity, relatively high thermal expansion coefficients that reduce Young's modulus, and excellent hardness and toughness are some of these characteristics [16, 17]. A trial-and-error strategy is employed, which is labor-intensive, expensive, and ineffective by nature.

Statistical methods, such as a Taguchi Designs of Experiments (DOE) technique [18], can greatly benefit process optimization by lowering the number of trials needed. The aforementioned strategy is an advanced design of experiments (DOE) method that may be used to simulate and assess the effect of modified elements on the performance outcome [19].

This technique aims to identify the most significant key variables (also known as control features) and their associated values. The researcher can determine the best configuration of control variables to produce the needed mean response value while limiting variability by computing the signal-to-noise ratio, which indicates design stability. The viability of using this technique to dip coat YSZ particles from fluid suspensions has been supported by recent research [20], proving this claim.

The study used multivariate assessment of variation (MANOVA) and least-squares regression analysis to determine the optimal combination of control parameters (concentration, temperature, quantity of grinding, and deposit length) that would maximize deposit weight while minimizing variability. The inclusion of microstructural analysis served as more data to bolster these findings. Electrochemical studies assessed the corrosion characteristics of several metal substrates coated with protective layers utilizing different coating processes [21].

2. Experimental

2.1 materials

Commercial pure Ti grade 2 bars were supplied by Baoji Jinsheng Metal Material Co., Ltd. And were cut to 10 mm in diameter with 2 mm thickness. They were ground with different grits (250, 280, and 400) with SiC papers. The samples were degreased with acetone and washed with deionized (DI) water. Zirconia-Yttria (ZrO_2 + 3 mol% Y_2O_3, 20–50 nm, purity of 99.5%, spherical white color, bulk density 0.6–1 g/cm^2) purchased from Nano Amor was used to prepare functionally graded material coatings. PVP (medium molecular weight with a degree of deacetylation of about 85% soluble in 1% acetic acid) and P_2O_5 were purchased from Sigma Aldrich.

2.1.1 Suspension preparation for dip coating

The procedure. Three distinct mixtures, each with a different concentration of YSZ particles, have been produced to determine the appropriate adhesion and coating thickness (10, 15, and 20% weight). First, a solution containing 5% water, 1% acetic acid, and 94% ethanol was used to dissolve 0.50 g/L of YSZ, 0.1 g of polyvinyl polymer PVP, and 0.5 g of P_2O_5. The procedure started at this point. The 50 ml backer was then filled with the YSZ nanopowder, and all of the suspensions were deagglomerated for 24 hours using a magnetic stir. The following thirty minutes were spent using a treatment with a very potent sonicator (ultrasonic processor speed, MIXSONIX, founded in New York, United States). Using a pH tester 818 and acetic acid, the mixture's pH level was lowered to 4 - 4.5 before the coating began. Prior to the procedure, this was done.

2.1.2 Suspension preparation for EPD

The process of making the aqueous solution is crucial to the EPD process. Three solutions with varied YSZ nanopowder percentages (10, 15, and 20 wt%) are shown to choose the optimal adhesion and coating thickness. First, 0.50 grams of chitosan per liter were dissolved in a solution of 94% ethanol, 5 % distilled water, and 1% acetic acid. The 50 ml suspension vial was then filled with YSZ nanopowder, and all suspensions were then deagglomerated using a magnetic stirrer for 24 hours. Before being coated, the material had been treated for 30 minutes with a high-frequency sonicator (ultrasonic processors, MIXSONIX Incorporated, New York, USA). The pH range of the solution (4- 4.5) was changed using an acetic acid pH tester and the pH 818 meter.

2.1.3 Dip coating

Dip coating involves submerging a substrate into a container filled with coating material, then withdrawing the component from the container and allowing it to drain. The covered object may then be dried by the process of forced drying. It is a commonly used method for producing materials with thin film coatings, in addition to the spin coating technique. Three solutions were created with varied YSZ nanopowder concentrations (10, 15, and 20% wt%) to evaluate the optimal adhesion and coating thickness. The mixtures were heated to various temperatures (30, 45, and 60°C) using a hot rod with a magnetic agitator and vigorous mixing. The sample was carefully immersed in the mixtures for 5, 10, and 15 seconds before being removed and allowed to dry. Repeating the process created a second coating, which was then left to air-dry.

2.1.4 Electrophoretic deposition

EPD industrial processes include Electrocoating, cathodic electrodeposition, electrophoretic coating, and electrophoretic painting. This process is distinguished by the migration of colloidal particles dispersed in a liquid medium under the influence of an electric field (electrophoresis) and their deposition on an electrode. All colloidal particles that can form stable suspensions and convey a charge can be utilized in electrophoretic deposition. This category comprises polymers, pigments, dyes, ceramics, and metals. In a 50 ml beaker, the readily available Ti, Ti-13Zr-13Nb (anode), and 316 L (cathode) electrodes were positioned 10 mm apart. A variety of voltages (40, 50, and 60), deposition periods (3, 5, and 7 min), and YSZ nano-powder concentrations (10, 15, and 20 wt%) were used to deposit the coating. The Taguchi technique was utilized to enhance the properties of the EPD coating, and the adhesion test and thickness were employed as the input and output data, respectively. To improve adhesion, each sample was dried in the oven for 10 minutes before being sintered for roughly 25 minutes at 200°C.

2.2 Characterization

2.2.1 Adhesion test by tip test analysis

According to the literature review, there are more than 250 techniques to measure how effectively coatings stick to substrates. The pull-off, tape tear, nano-indentation, and abrasion tests are frequently used to evaluate adhesion strength. Given that test methodologies are influenced by coating and substrate factors, an effective testing method will likely replicate the usage stress. For coatings thicker than 20 µm, the pull-off test process should be employed, and it should take into consideration the detrimental impacts of epoxy adhesive penetration and uneven coating flaking. The tape peel-off test also has limitations, such as its non-quantitative nature and lack of reproducibility. [21] The tip test is a reliable, repeatable, and quantitative adhesion testing tool that can penetrate coating systems without using epoxy adhesive. On YSZ coatings, a qualitative abrasion test was performed. ImageJ software was used to examine data stored on the computer. The investigation entailed applying a force of 1 N to the adhesion strength using a 5 mm stroke width and a 0.5 mm/s ramp scratch speed. Crosshatch tape was used to assess the adhesion strength between the coatings and the base material in accordance with ASTM standard D3359. The test required inserting and removing the tape from the coating's surface at the grit junction after making five extensive cuts on the specimens in each direction (with at least 4 mm separating each cut from the next).

2.2.2 The analysis of optical microscopy images and FE-SEM-EDAX

The CP-Ti's YSZ coating's thickness was measured using an optical microscope and digital camera. At least three measurements were made on the coated sample at various locations to establish the mean coating thickness. We examined the microstructure, morphology, and elemental composition of the YSZ coating we created using a scanning electron microscope with elemental analysis instruments (FE-SEM-EDAX, FEI, and Axia Chami-SEM). The sessile dropping technique and an automated dropped shape analysis (SL200B, United States) were used to calculate the water's contact angle. We evaluated duplicate samples of each composite coating. An X-ray diffraction equipment (XRD-6000, Shimadzu) was used for the phase analysis, scanning at a rate of 3° min1 and with a step width of 0.05° every 2° from 10° to 90°.

The Nano 90 zeta potential sizer (Malvern Technologies) with dynamic light scattering was used to assess the zeta potentials of the suspensions. The suspensions underwent ultrasonographic treatment before the trials to ensure they were evenly dispersed. AFM 3-D interface imaging in tapping mode and the MOUNTAINS9 software was especially used to assess the surface texture and thickness of the coated interface. The probe had a thin silicon tip that was attached to a lever made of nitride. The surface area that was taken into account was only 40 µm x 40 µm in size. A CCD camera and a contact angle measuring device (Creating Nanotechnology Tech., Model: CAM110P, Serial No. 113031201804W) were used for the wettability testing. This test technique enables evaluating and measuring the coated substrate's wettability properties, also known as its hydrophobic properties. Deionized water and the solid surface's contact angles are measured to achieve this. After analyzing the samples, the relevant contact angle values were determined and then averaged.

2.2.3 Corrosion test

This study uses in-vitro testing to assess the corrosion resistance of dip coatings and electrophoretically deposited YSZ coatings. Time measurement is used to assess the open circuit potential (OCP). Corrosion testing may be divided into two different categories. The first technique used to evaluate the corrosion characteristics in the samples is Tafel extrapolation. The link between the likelihood of pitted corrosion denoted as Epp, and the likelihood of pitted corrosion current density, designated as Ipp, indicates the reversal of anodic polarization. A 10 by 2 millimeter sample group was used to study corrosion resistance. Prior to being examined in a simulated bodily fluid (SBF) solution, the coated specimens were not subjected to grinding and polishing, whereas the uncoated specimens were. The reference electrode was made of Ag /AgCl, whereas the counter electrode

was made of a platinum filament. Using in vitro research, a modified simulation of body fluid known as revised simulated body fluid (r-SBF) was used to assess the efficacy of coatings in preventing corrosion. The SBF solution, which had a pH of 7.4, contained the following ions: sodium (Na^{+}), which was present at a concentration of 142.0 millimolar (mM). Potassium (K^{+}) was present at a concentration of 5.0 mM, magnesium (Mg^{2+}) was present at a concentration of 1.5 mM, calcium (Ca^{2+}) was present at a concentration of 2.5 mM, and bicarbonate (HCO^{3-}) was present. The research's target potential range was designed to be between -1000 mV and +1500 mV. A WENKING M, LAB model potentiostat was used for an additional test. Germany is where the electrochemical system was made. Using potentiostat software, the analysis of data values (current and voltage) yielded the corrosion current intensity (icorr) and corrosion potential (Ecorr) values.

3. Results and Discussion

3.1 Selection of Optimum Conditions for Dip Coating

This research selected the YSZ concentration, the applied temperature, the grid of samples, and the deposition duration as the control variables. The levels of significance for each component are shown in Table 1. An orthogonal Taguchi arrangement of the L9 type was created using these three controls. L denotes "Latin square," and "9" denotes the number of times the trials were carried out. The L9 orthogonal array's design requirements are shown in Table 2. The four-parameter levels used were the YSZ concentration, milling degree, temperature, and time. The average result and standard deviation were collected after at least three replications of each run. The statistical application MINITAB 15 was used to carry out the analysis. Notably, the approach used removes 160 dip coating cycles for a full factorial design, saving a substantial amount of time and money.

The Taguchi technique was used to determine the ideal parameters (temperature, duration, concentration, and degree of grinding) to deposit coating layers of YSZ for titanium alloy Table 1. Thickness and roughness are the two forms of output data needed for this investigation. Table 2 lists the variables that are employed in dip coating.

Table 1: Parameters used in dip coating

Temperature	30	45	60
Time, sec.	5	10	15
Concentrations %	20	15	10
Grits of grinding	400	280	250

3.1.1 Taguchi Results

Using the Taguchi statistical method, the optimal conditions for YSZ layer preparation on CP-Ti substrates were determined after suspension prep for YSZ preparation. Since the objective of YSZ layer preparation is to attain the highest adhesion and coating thickness, the signal-to-noise ratio (S/N) was used to determine the optimal values of temperature (T), time (t), concentration (C), and grinding degree, as shown in Table 4 and Figure 1. Using the Taguchi design (L9), these values were determined for the thickness and adhesion measurement results of the YSZ layer. Table 1 shows the optimal conditions for YSZ coating thickness and adhesive for Ti alloy when dip coating is utilized.

3.1.2 Analysis of YSZ deposition on CP-Ti

According to Table 2, commercially pure Ti can generate a wide range of thickness and adhesion values with varying degrees of variability. The SNs ratio thesis (larger is superior) indicates that the experiment via the highest SNs ratio value has implicitly higher quality. The thickness and adherence of YSZ layer coatings were determined using the specified Taguchi method. Sample 9 has larger thickness, adherence, and SNS ratio values, as shown in Table 2. Experiment (9) yielded the greatest thickness (60µm) with 60 Temp, 15 sec, 15% C, and 250 grain silica pulverized. As displayed in Figures 1 and 2, the optimal conditions for forming the YSZ film are 60 °C, 10 seconds, 10% C, and a silica pulverization of 250 grains. The solution's effective particle dispersion From Tables 3 and 4, it was determined that the temperature (37.14%), time (31.83%), degree of milling (3.20%), and concentration (27.53%) influence the thickness of the YSZ deposit layer the most. Figure 5 (1-9) depicts a cross-section of nine YSZ coating samples. Temperature (63.81%), time (4.81%), degree of grinding (10.92%), and concentration (20.46%) are listed in Tables (5, 6) for YSZ adhesion. Figure 6 (1-9) depicts the removal area for YSZ coating layers for pure commercial Ti.

Table 2: Signal-to-noise (S/N) ratio for commercial Ti alloy

	Temp	T	C	D	Th.	Ad.	SRNA1	MEAN1	SRNA2	MEAN2
1	30	5	10	250	34	16.24	30.6296	34	-24.211	16.24
2	30	10	15	280	37	30.90	31.3640	37	-29.799	30.90
3	30	15	20	400	28	36.58	28.9432	28	-31.264	36.58
4	45	5	15	400	33	19.33	30.3703	33	-25.724	19.33
5	45	10	20	250	44	22.59	32.8691	44	-27.078	22.59
6	45	15	10	280	56	22.10	34.9638	56	-26.887	22.10
7	60	5	20	280	32	15.93	30.1030	32	-24.044	15.93
8	60	10	10	400	62	5.76	35.8478	62	-15.208	5.76
9	60	15	15	250	60	7.87	35.5630	60	-17.919	7.87

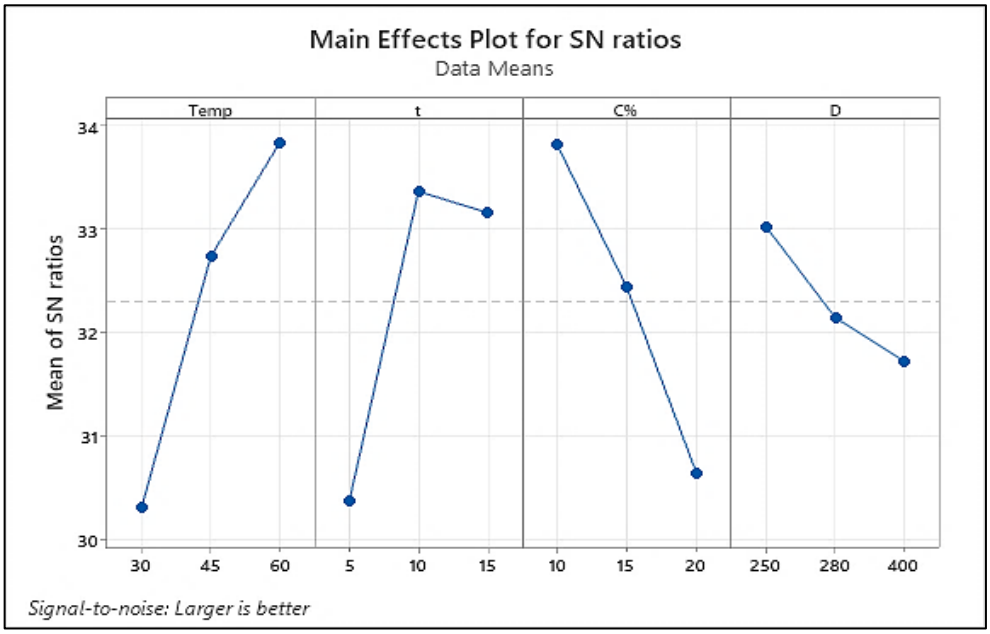

Figure 1: S/N ratio for thickness (commercial Ti)

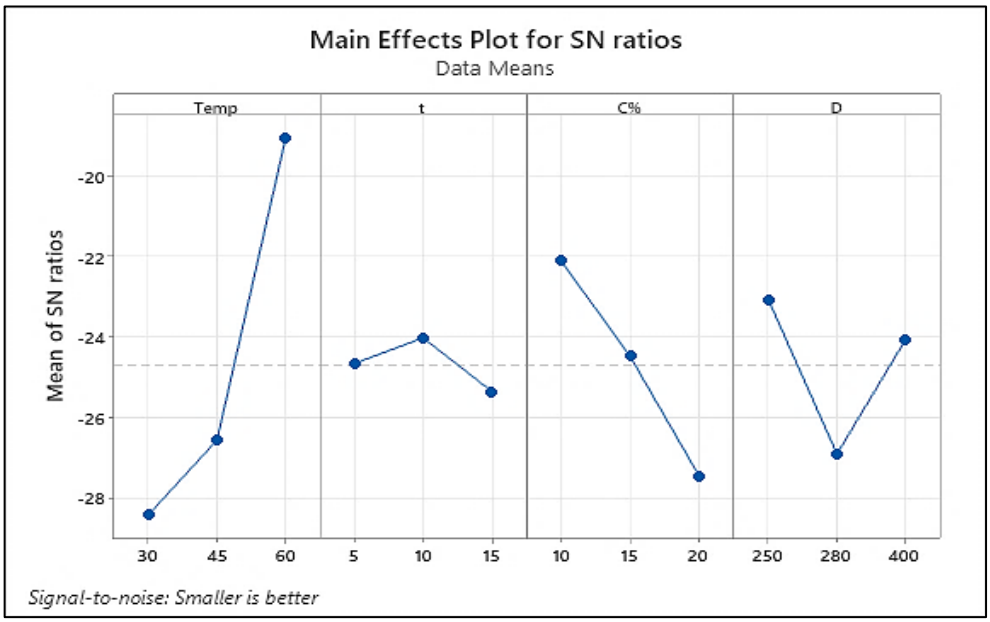

Figure 2: S/N ratio Adhesion (commercial Ti)

Table 3: Rank of controlled factors for the thickness of the YSZ layer for commercial pure Ti Response Table for Signal-to-Noise Ratios

Level	Temp	t	C%	D
1	30.31	30.37	33.81	33.02
2	32.73	33.36	32.43	32.14
3	33.84	33.16	30.64	31.72
Delta	3.53	2.99	3.18	1.30
Rank	1	3	2	4

Table 4: ANOVA for the thickness Of the YSZ layer for Commercial pure Ti

Source	DF	Adj SS	Adj MS	Contribution
Temp	2	513.56	256.78	37.14%
t	2	440.22	220.11	31.83%
C	2	384.89	192.44	27.83%
D	2	44.22	22.11	3.20%
Error	0			
Total	8	1382.89		100 %

Table 5: Rank of controlled factors for Adhesion of the YSZ layer for commercial pure Ti

Level	Temp	t	C%	D
1	-28.43	-24.66	-22.10	-23.07
2	-26.56	-24.03	-24.48	-26.91
3	-19.06	-25.36	-27.46	-24.07
Delta	9.37	1.33	5.36	3.84
Rank	1	4	2	3

Table 6: ANOVA for the Adhesion of YSZ layer for Commercial pure Ti

Source	DF	Adj SS	Adj MS	Contribution
Temp	2	500.99	250.49	63.81%
t	2	37.76	18.88	4.81%
C%	2	160.67	80.33	20.46%
D	2	85.66	42.83	10.92%
Error	0			
Total	8	785.08		100%

3.2 Selection of Optimum Conditions for EPD

In these experiments, the concentration of YSZ, the applied voltage (at the same distance between electrodes), the specimen grid, and the deposition time were chosen as the control parameters. The levels of each component are displayed in Table 7. Using these three control elements, an orthogonal Taguchi array of type L9 was constructed (L stands for Latin square, and 9 represents the number of trial repetitions). Table 8 displays the specifics of the L9 diagonal array architecture. Four parameters were utilized: YSZ concentration, milling intensity, voltage, and time. At least three test repetitions were conducted, and the mean and standard deviation were recorded. MINITAB 15 statistical software was used to conduct the analysis. It is essential to note that the employed method eliminates 180 EPD cycles for complete factorial design, resulting in significant time and cost savings.

Taguchi analysis was used to determine the optimal conditions (voltage, duration, time, concentration, and degree of pulverization) for depositing YSZ-coated layers on titanium alloy table 7. This investigation requires two types of output data: thickness and texture. Table 8 enumerates the variables utilized in the EPD.

Table 7: Parameters used in EPD

Voltage	20	40	60
Time, min.	3	5	7
Concentrations %	10	15	20
Degree of grinding	250	280	400

3.2.1 Taguchi Results

Following suspension preparations for YSZ preparation, the Taguchi statistical technique was used to determine the optimal conditions for YSZ layer preparation on commercially available Ti substrates. Four optimal values of voltage (V), time (t), concentration (C), and degree of grinding were selected based on the signal-to-noise ratio (S/N), as shown in Table 4 and Figure 1and 2, using the Taguchi method (L9) for thickness and adherence measurement results of YSZ layer with coating thickness using DC. This is because the YSZ layer of the formulation seeks to achieve the highest adhesion and coating thickness. Table 7 illustrates Ti alloys' optimal YSZ coat thickness and adhesive when employing EPD with DC.

3.2.2 Analysis of YSZ deposition on CP-Ti

Table 8 showed that different degrees of variability were used to achieve a wide range of both thickness and adherent measurements for commercially pure Ti. The experiment with the largest value of the SNs ratios implicitly has the superior quality, according to the SNs ratio hypothesis (bigger is better). The Taguchi technique determined the YSZ coating layers' thickness and adherence. Table 8 demonstrates that sample 9 has greater thickness, adherence, and SNS ratio values. The experiment (9) using 60 V, 7 min, 15% C, and 250 grit silica grinds produced the thickest layer (102 µm). However, as demonstrated in Figures 3 and 4, the ideal conditions for deposition of the YSZ film are 60V, 7 min, 15% C, and 400 grit silica grinds. The solution's effective particle dispersion Tables 9 and 10 revealed that the voltage (78.27%), duration (13.18%), degree of grinding (5.92%), and concentration (2.63%) are the factors that are most influenced by the deposit YSZ layer's thickness, respectively. The cross-section of nine samples with YSZ coatings is shown in Figure 7 (1-9). According to Tables 11 and 12, YSZ represents the voltage (71.88%), time (11.50%), degree of grinding (13.29%), and concentration (3.34%) for adhesion, respectively. The removing area of YSZ layer coatings for commercial pure Titanium is shown in Figure 8 (1-9).

Table 8: Signal-to-noise (S/N) ratio for commercial Ti alloy

	V	T	C	D	Th.	Ad.	SRNA1	MEAN1	SRNA2	MEAN2
1	20	3	10	250	51.0	20.78	34.1514	51.0	-26.35	20.78
2	20	5	15	280	52.0	29.28	34.3201	52.0	-29.33	29.28
3	20	7	20	400	69.0	19.94	36.7770	69.0	-25.99	19.94
4	40	3	15	400	62.5	11.99	35.9176	62.5	-21.57	11.99
5	40	5	20	250	47.0	24.51	33.4420	47.0	-27.78	24.51
6	40	7	10	280	63.0	18.71	35.9868	63.0	-25.44	18.71
7	60	3	20	280	79.0	11.00	37.9525	79.0	-20.82	11.00
8	60	5	10	400	93.0	6.74	39.3697	93.0	-16.57	6.74
9	60	7	15	250	102.0	5.68	40.1720	102.0	-15.08	5.68

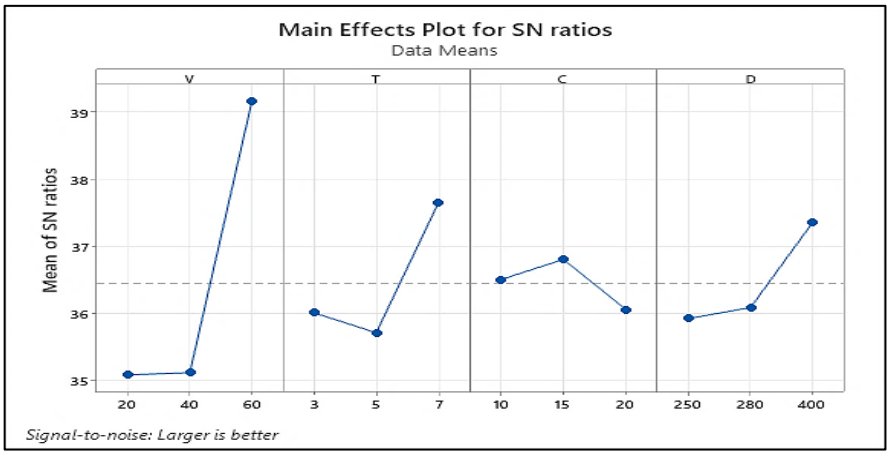

Figure 3: S/N ratio for thickness (commercial Ti)

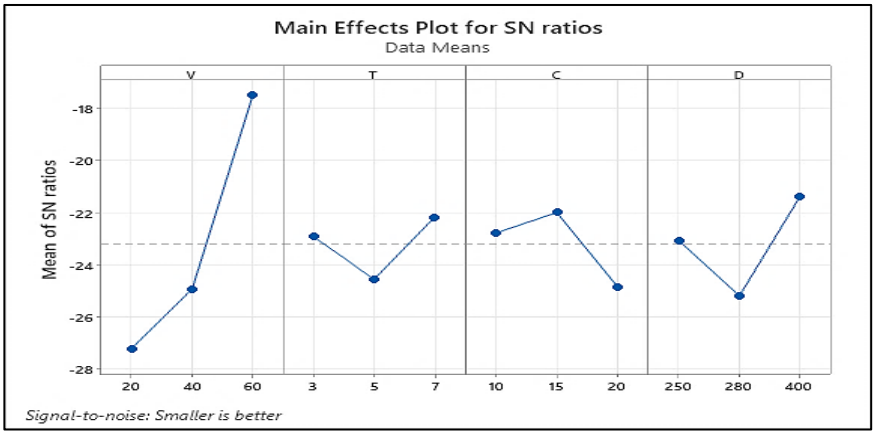

Figure 4: S/N ratio Adhesion (commercial Ti)

Table 9: Rank of controlled factors for the thickness of the YSZ layer for commercial pure Ti

Level	V	T	C	D
1	35.08	36.01	36.50	35.92
2	35.12	35.71	36.80	36.09
3	39.16	37.65	36.06	37.35
Delta	4.08	1.93	0.75	1.43
Rank	1	2	4	3

Table 10: ANOVA for the thickness of the YSZ layer for Commercial pure Ti

Source	DF	Adj SS	Adj MS	contribution
V	2	2300.72	1150.36	78.27%
T	2	387.39	193.69	13.18%
C	2	77.39	38.69	2.63%
D	2	174.06	87.03	5.92%
Error	0			
Total	8	2939.56		100%

Table 11: Rank of controlled factors for Adhesion of the YSZ layer for commercial pure Ti

Level	V	T	C	D
1	-27.23	-22.92	-22.79	-23.08
2	-24.93	-24.56	-22.00	-25.20
3	-17.50	-22.17	-24.87	-21.38
Delta	9.73	2.39	2.87	3.82
Rank	1	4	3	2

3.3 Corrosion Results

The best YSZ coatings for CP-Ti were found using the open circuit potential (OCP)-time technique for both coating procedures. For the best coatings, measurements of the potential in relation to time are used to understand the electrochemical corrosion behavior. In newly made simulated body fluid (SBF), the potentiodynamic polarization curves of uncoated CP-Ti alloys and YSZ-coated CP-Ti alloys were evaluated at 37°C. By extrapolating the anodic and cathodic branches of the polarization curves to the corrosion potential, the corrosion current (ICorr) was computed from the polarization curves (Figure 9). Table 12 shows the corrosion potential, corrosion potential density, and corrosion rate (mpy). The corrosion rate considerably lowers as the surface of the Titanium receives the finest coating. When CP-Ti coatings are applied using EPD with YSZ, the corrosion rate is lower than when CP-Ti coatings are applied using dip coating. The cyclic polarization of CP-Ti alloys covered with YSZ is shown in Figures 10 (a,b and c). Due to the very small leakage of potentially dangerous metallic ions into the surrounding tissues, the exceptionally low corrosion rate is crucial in implant applications.

The aforementioned phenomenon was seen in uncoated CP-Ti alloys and composite coatings. [22] have also documented a congruent discovery in their study with coatings. Similarly, Zaveri et al. [23] have seen a parallel phenomenon in their investigation of composite coatings on implant materials immersed in simulated human fluids. According to the findings of Tabesh et al. [24], it is proposed that the observed reduction in corrosion current may be related to the coating's role as a barrier, preventing the movement of corrosive ions.

Table 12: ANOVA for the Adhesion of YSZ layer for Commercial pure Ti

Source	DF	Adj SS	Adj MS	contribution
V	2	377.67	188.836	71.88%
T	2	60.41	30.203	11.50%
C	2	17.53	8.765	3.34%
D	2	69.83	34.917	13.28%
Error	0			
Total	8	525.44		100.00%

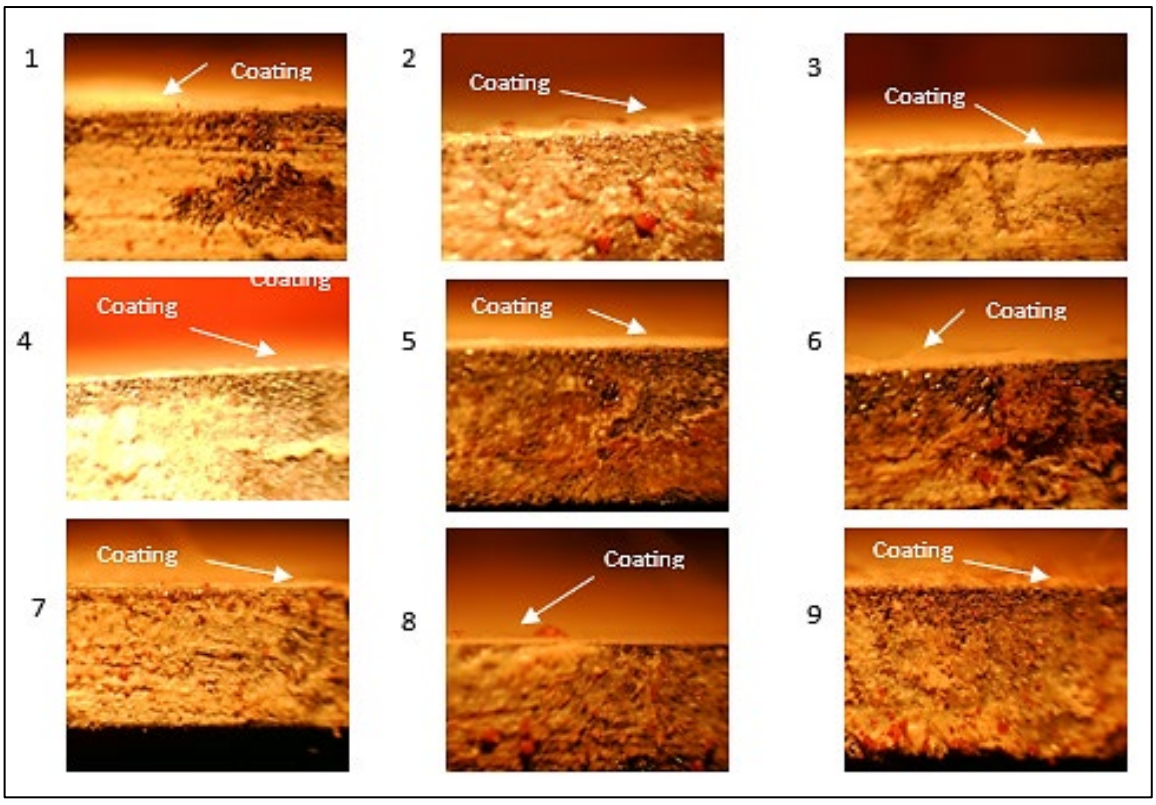

Figure 5: The YSZ coat layer on a cross-section of commercial pure Ti specimens by dip coating (10X)

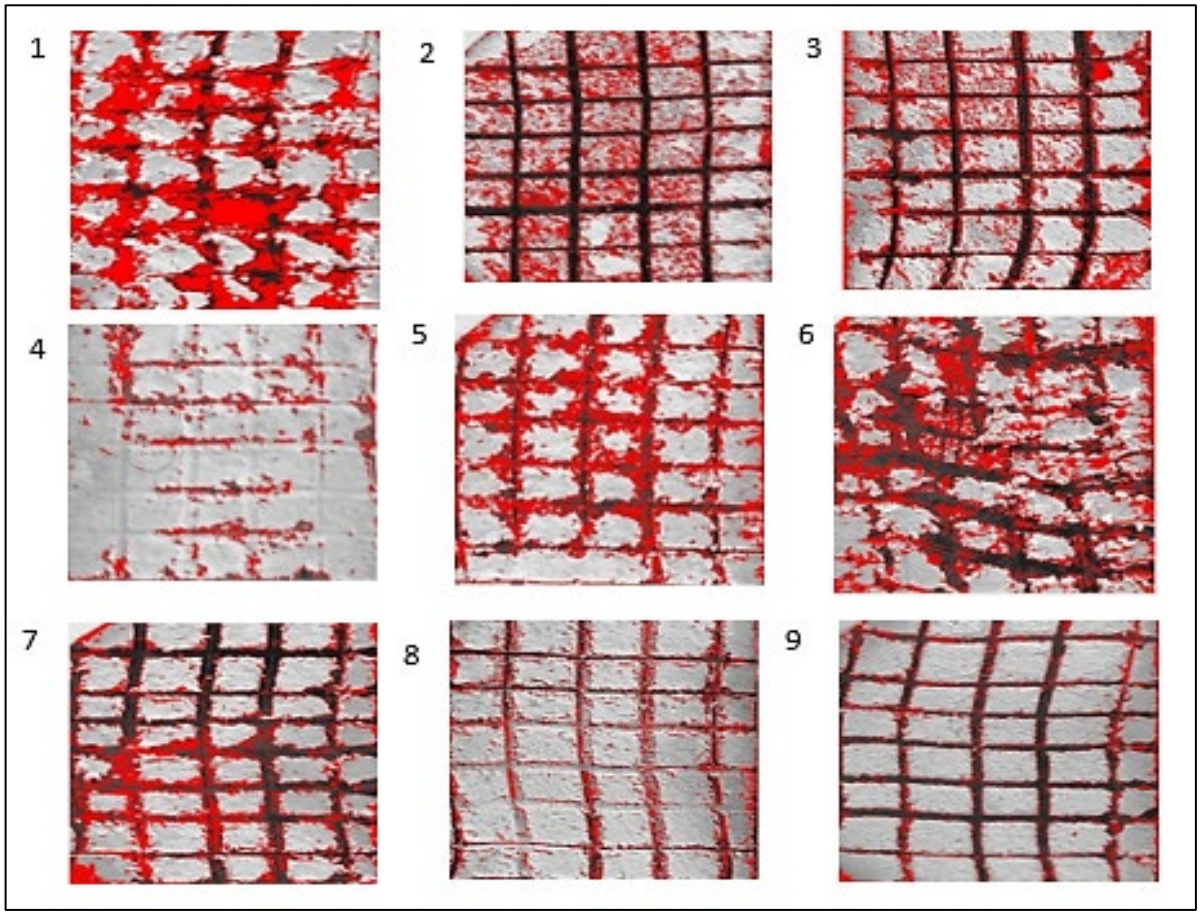

Figure 6: Area from YSZ coating layer removal for commercially pure Ti coated by dip coating

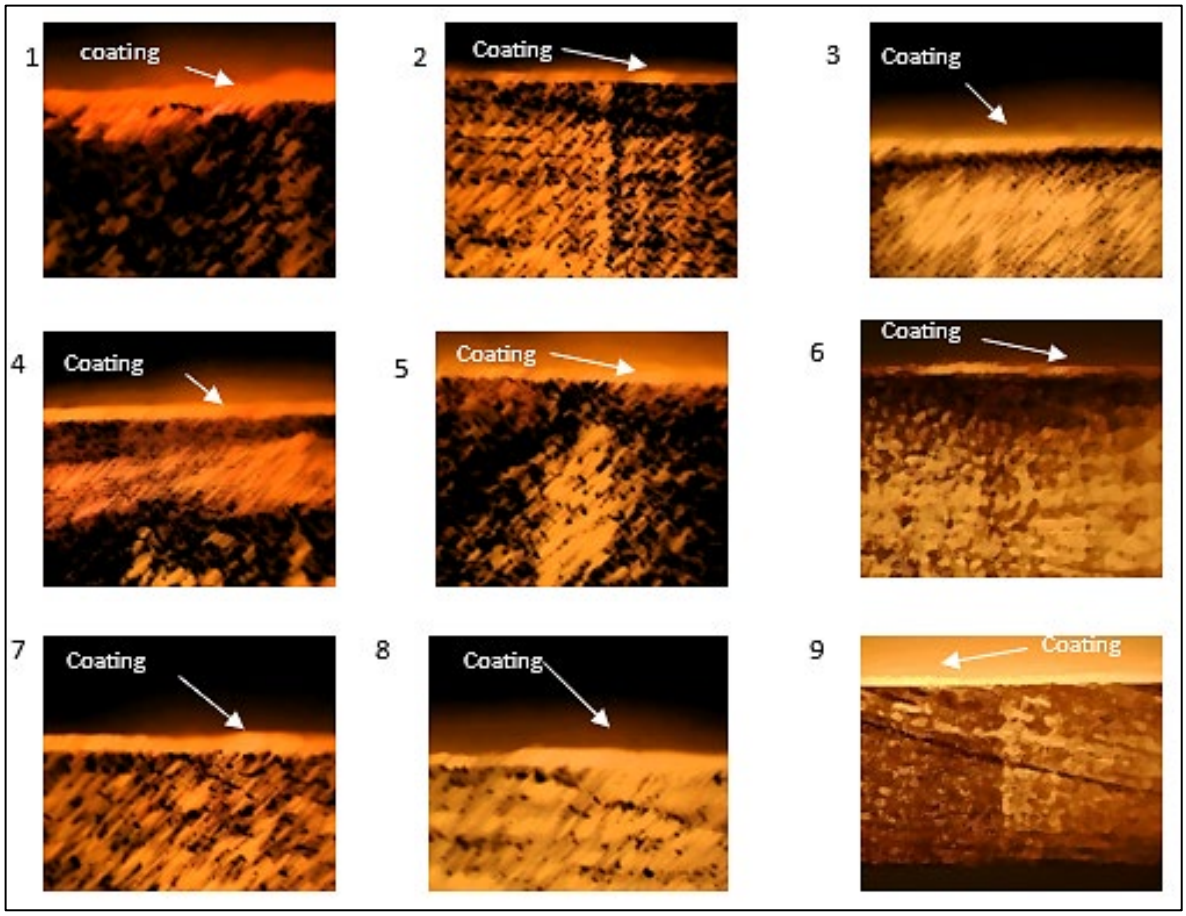

Figure 7: The YSZ coating layer on the cross-section of specimens for CP-Ti coated by EPD (10 X)

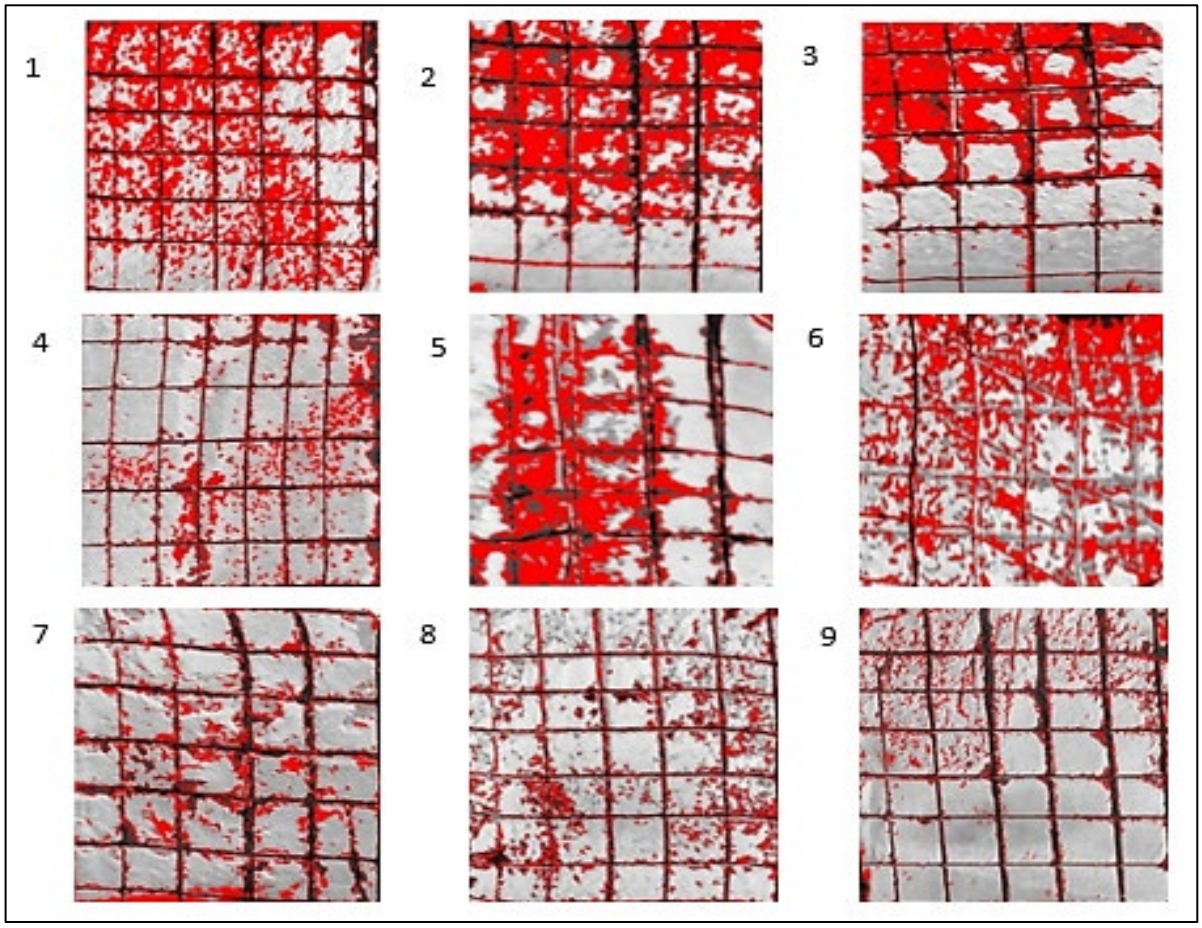

Figure 8: Removal area of YSZ coating layers for CP-Ti coated by EPD

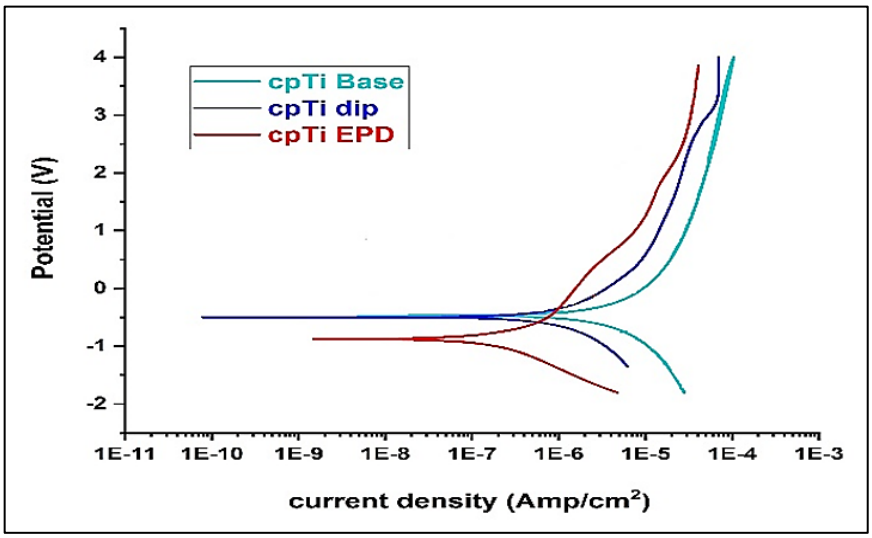

Figure 9: Polarization curves of uncoated and coated commercial pure-Ti

3.4 Surface Morphology

The images taken using field emission scanning electron microscopy (FE-SEM) to study CP-Ti alloys showed that the coating was uniform and compact, free of any obvious fissures. Additionally, identical particle sizes were observed in the coated layers, as shown in Figures 11 and 12.

Energy dispersive spectroscopy (EDS) was used to perform a chemical study on the CP-Ti alloys coated in a YSZ layer, as shown in Figures 13 (a) and (b), respectively. The findings of a phase analysis performed to identify the best coatings for CP-Ti alloy, both before and after the coating process, are shown in Figures 14(a) and (b).

To determine the crystalline structure and phase properties of nano-YSZ, an X-ray-ray fraction (XRD) investigation is used. The YSZ coating method was used on both coated alloys, which exhibited almost similar peak properties. Strong diffraction peaks may be seen in the X-ray diffraction (XRD) pattern of ZrO_2 at five different angles: 28.12°, 29.81°, 31.42°, 50.01°, and 59.34°.

The Miller indices m (-111), t (101), m (110), t (200), and t (211) are the discovered peaks' respective values. This suggests that zirconia exists in tetragonal and monoclinic phases. As shown in Table 13, the relevance of the magnitude of peak intensity commonly emerges as a noteworthy component within the context of composites. The presence of crystalline boundaries and the inherent crystalline structure considerably impact the stability of suspensions and the development of thick films.

Table 13: The corrosion current density, potential, and rate (mpy)

ITEM	E corr. (volt)	I corr. (Amp.)	Corr. Rate mmpy	βa	βc	OCP (volt)
Ti base	-0.483	1.193×10^{-6}	2.696×10^{-2}	0.252	0.257	-0.441
Ti dip	-0.497	4.612×10^{-7}	1.042×10^{-2}	0.220	0.197	-0.423
Ti epd	-0.879	1.341×10^{-7}	3.031×10^{-3}	0.223	0.232	-0.419

The occurrence of diffraction peaks at certain 2θ values, as shown in Table 14, indicates the presence of zirconium dioxide. This is well supported by the chemical makeup of the used alloy. With the aid of a constant flow of distilled water, the hydrophobicity or wettability of coated titanium alloy specimens is measured. This is done by determining the angles at which solids and liquids interact using optical contact angle equipment with a CCD camera.

The potential zeta is regarded as one of the most important variables in this situation. The parameter significantly affects (i) the solution's stability, (ii) the direction of particle migration, (iii) and (iv) the coating's density and homogeneity (v) [25, 26]. The zeta potential analyzer (ESA 9800, Matec Applied Science Corporation, USA) was used to calculate the zeta potential values of suspensions containing various concentrations of YSZ (20%,15%, and 10%). This finding shows that an increase in YSZ concentration causes a comparable increase in zeta potential values, measured at 30.13 mV and 24.06 mV, respectively.

The contact angles observed for both coated and uncoated CP-Ti samples were measured to be 117.484° based on the information shown in Figure 15. The contact angles were 58.418° and 64.867° for CP-Ti samples coated using the electrophoretic deposition (EPD) and dip coating techniques, respectively. These findings imply that a coating enhances the hydrophilicity of the CP-Ti surfaces. The argument makes the case that surfaces with hydrophilic characteristics are preferable to those with hydrophobic characteristics. There is a reference to the numerals 27 and 29. According to research done in vitro by Rausch-Fan et al. and Zhao et al., the hydrophilic properties of titanium surfaces substantially impact the differentiating of cells and the production of growth factors. The user has specified a range of numbers, particularly [27, 28]. Additionally, research on animals has demonstrated that on hydrophilic surfaces, osseointegration can start early [29].

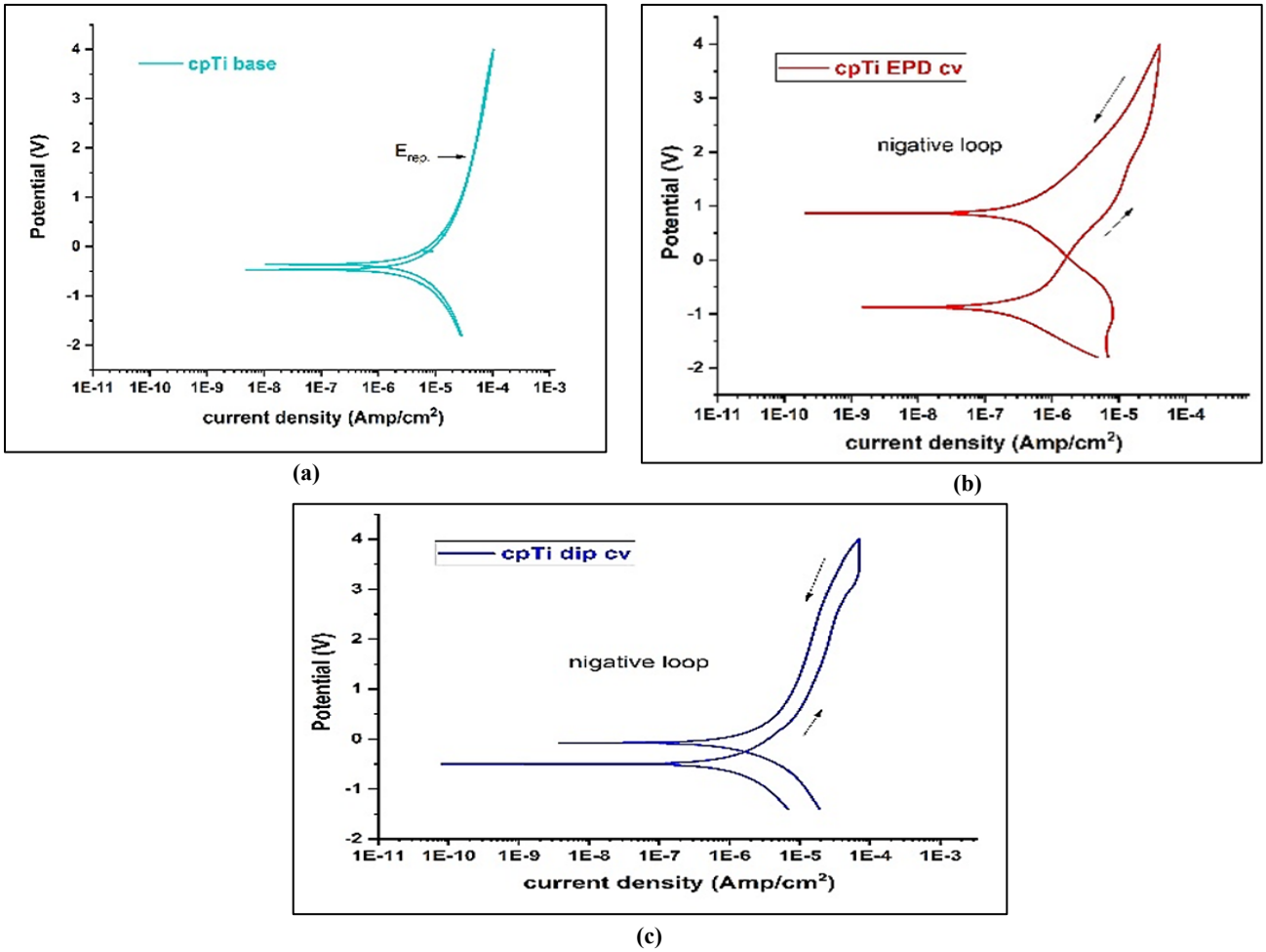

Figure 10: Cyclic polarization curves of (a) uncoated CP-Ti, (b) YSZ coated CP-Ti by EPD, (c) YSZ coated CP-TI by dip coating.

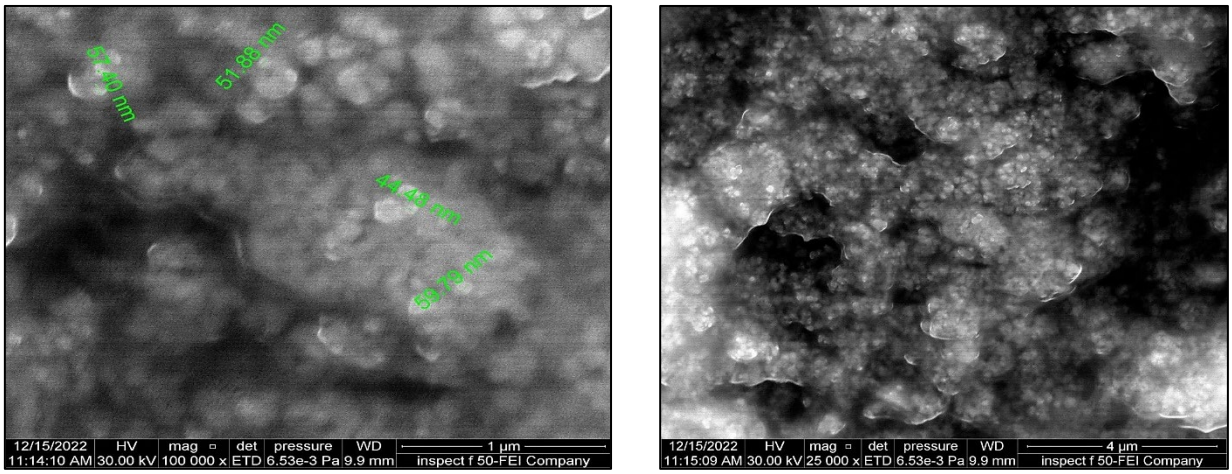

Figure 11: FE-SEM of coated CP-Ti by dip coating

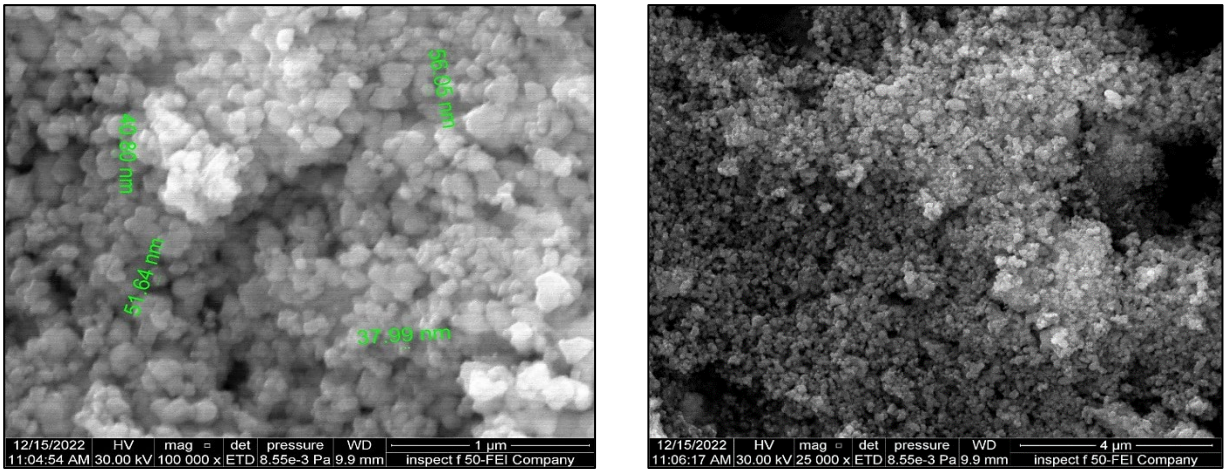

Figure 12: FE-SEM of coated CP-Ti by EPD

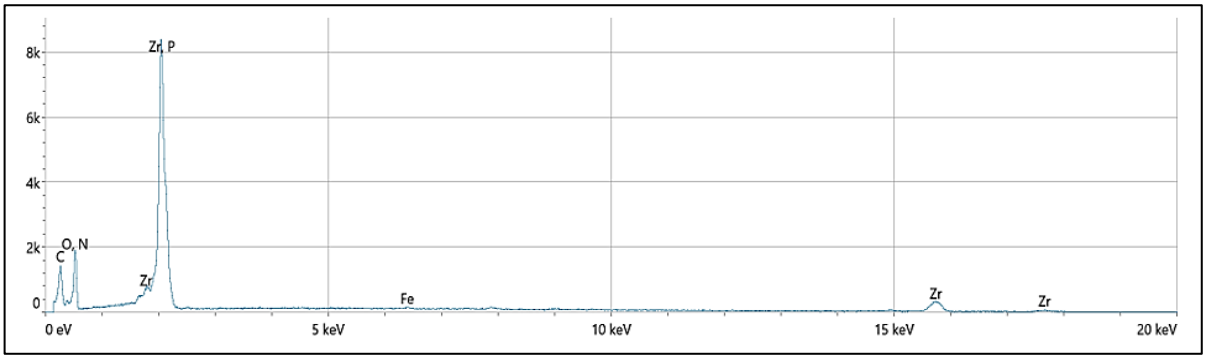

(A)

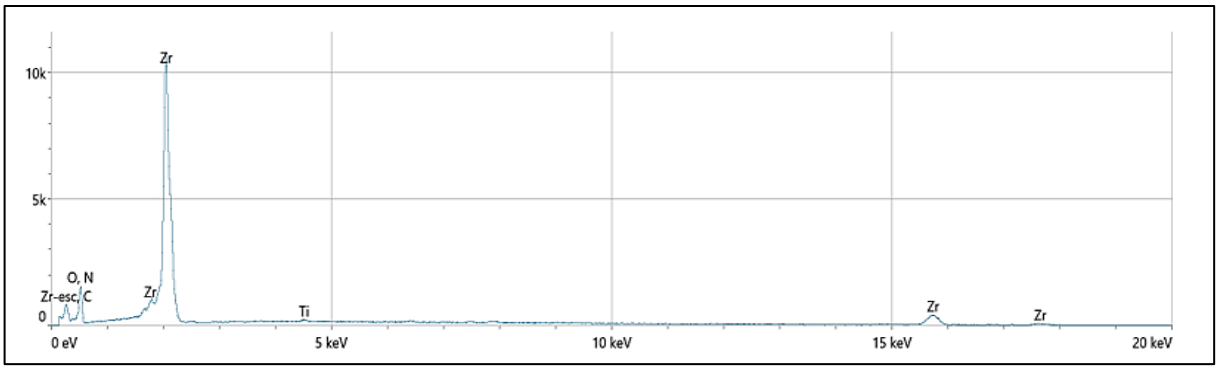

(B)

Figure 13: The EDS of (A) YSZ-coated CP-Ti by Dip coating and (B) YSZ-coated CP-Ti by EPD

Table 14: XRD analysis

Peak no.	2θ	material	phase	hkl	ICDD
1	24.10	ZrO_2	monoclinic	110	37-1484
2	28.12	ZrO_2	monoclinic	-111	37-1484
3	29.81	ZrO_2	tetragonal	101	42-1164
4	31.42	ZrO_2	monoclinic	111	37-1484
5	34.81	ZrO_2	tetragonal	110	42-1164
6	40.69	ZrO_2	monoclinic	112	37-1484
7	50.01	ZrO_2	tetragonal	200	42-1164
8	55.38	ZrO_2	monoclinic	310	37-1484
9	59.34	ZrO_2	tetragonal	211	42-1164

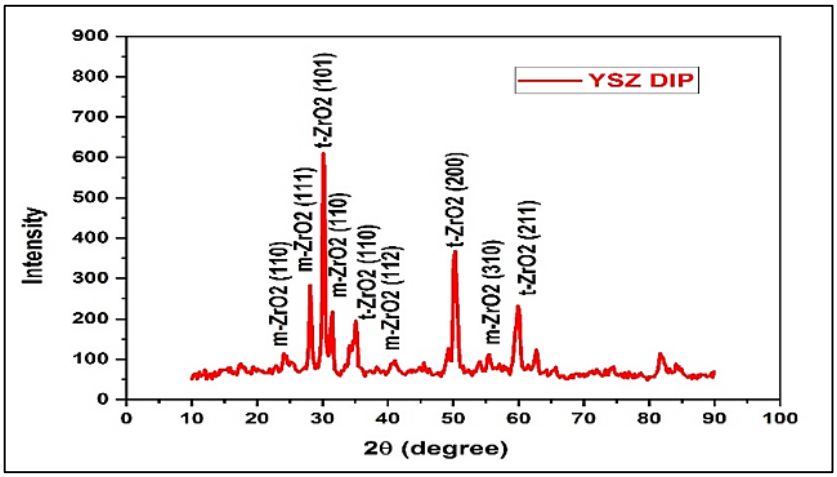

(a)

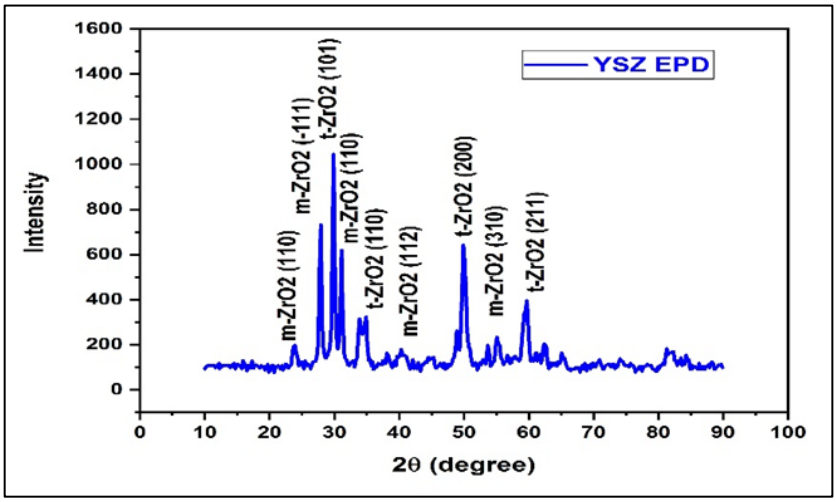

(b)

Figure 14: a) XRD for YSZ coated CP-Ti by Dip coating b) XRD for YSZ coated CP-Ti by EPD

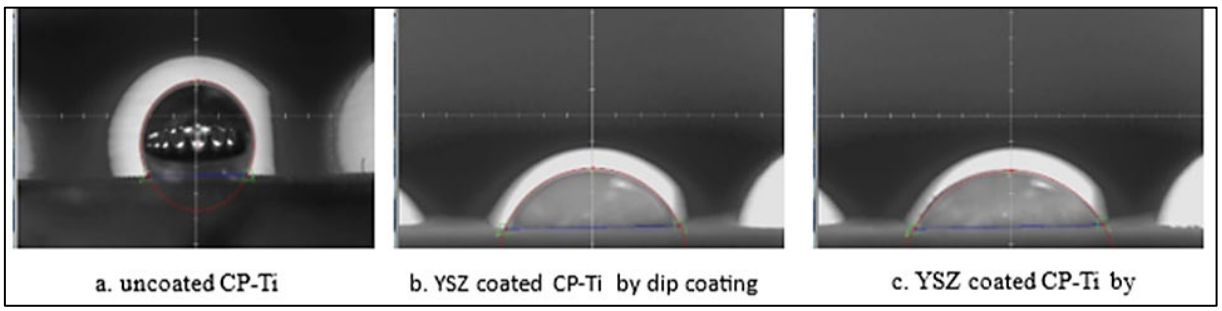

Figure 15: Water contact angle measurement

Roughness is a property that describes the imperfections that include both troughs and peaks in the surface profile of an implant (see Figure 16 a and b). This characteristic significantly impacts how cells respond to the implant's surface, including

how they proliferate, differentiate, and adhere. As shown in Table 15, the object's dimensions were determined using a micrometer instrument, and the coating layers' nano-roughness was examined using an atomic force microscope (AFM). The roughness measurement of Cp-Ti coated by EPD was observed to be less than the roughness measurement of Cp-Ti coated by dip coating process due to the layer of coated sample by EPD being more uniform and approximately had the same thickness along the layer compared with the coated sample by dip coating process and that conformed by the measurement of contact angles for both coated sample.

Table 15: Roughness measurement by micrometer and AFM

Samples	AFM nano-scales	micrometer
Coated YSZ CP-Ti by Dip coating	106.4 Nm	6.422 µm
coated YSZ CP-Ti by EPD	68.06 Nm	0.746 µm

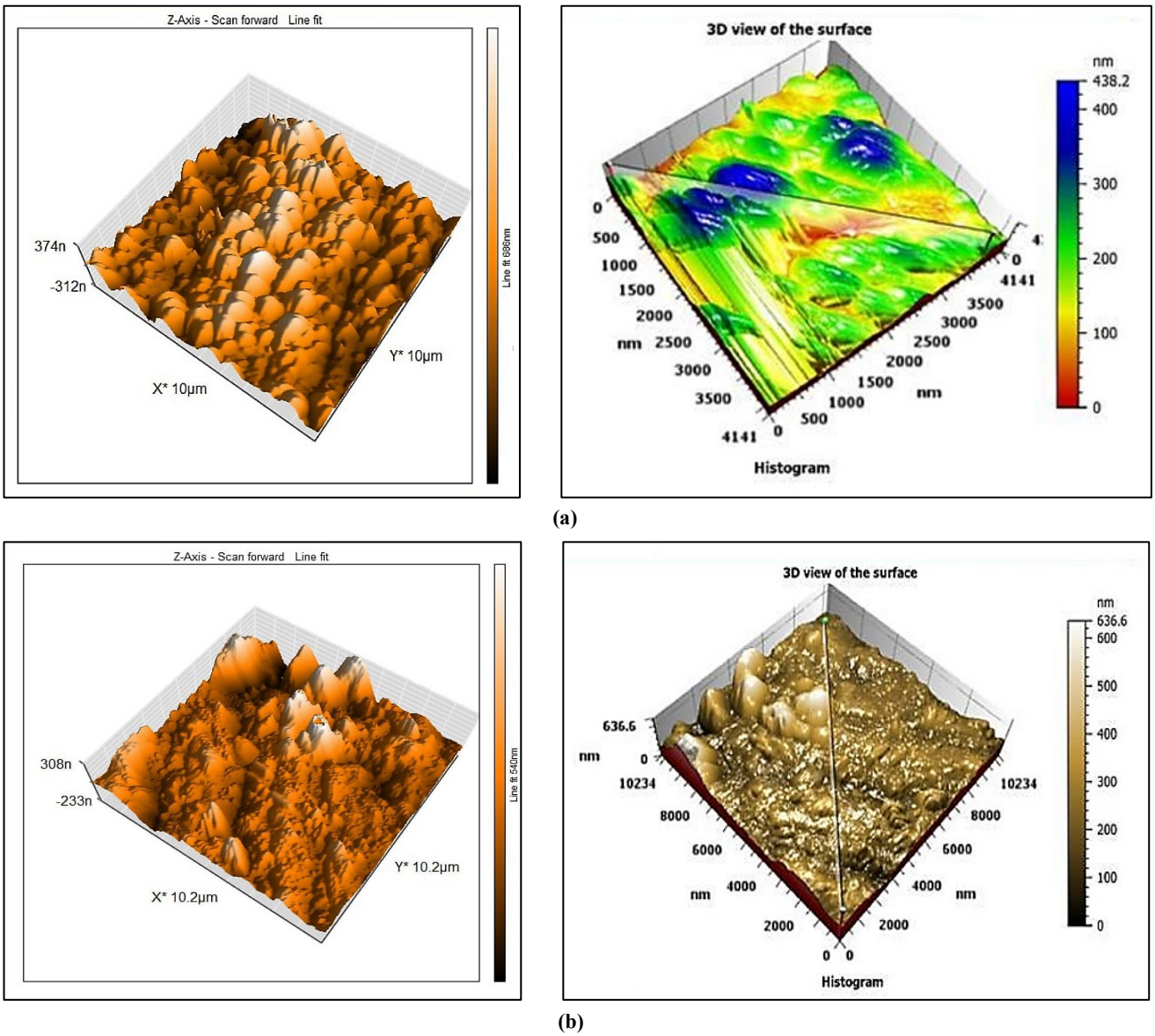

Figure 16: AFM images show topographies of (a) CP-Ti coated by EPD (b) Ti-13Zr-13Nb coated by dip coating

4. Conclusion

1) EPD has successfully coated The titanium alloy CP-Ti with the YSZ coating. The adhesion and thickness parameters provide the best conditions for depositing the YSZ coating by EPD on the titanium alloy CP-Ti.
2) The adhesion and thickness characteristics establish the appropriate conditions for dip coating YSZ coated on CP-Ti. On CP-Ti, the YSZ coating was effectively deposited.
3) The optimal deposition parameters for the YSZ layer via dip coating were found to be 60°C, 10 seconds, 10% C, and 250 grinding for the CP-Ti alloy.
4) After the data was evaluated, it was discovered that 60 V, 7 minutes, 15% C, and 400 degrees of grinding provided the ideal conditions for forming the YSZ layer for the CP-Ti alloy.

5) It was discovered that the YSZ layer for CP-Ti alloys coated by both processes is homogenous and dense. It is a continuous coating layer by examining the samples' microstructure on the alloy substrate.
6) Water contact angle studies on sample materials revealed that coated CP-Ti alloys, which are renowned for being hydrophilic, had a YSZ coating surface of 58.418° as compared to dip-coated alloys, which have an angle measurement of 68.867°.
7) The surface morphology investigation carried out using AFM reveals that the CP-Ti alloy coated by EPD displays lower surface roughness than the coated dip coating.
8) Both coated CP-Ti alloys enhanced corrosion resistance in Ringer's solution at 37°C. However, the coated CP-Ti alloy by EPD demonstrated greater corrosion resistance than the coated CP-Ti alloy by dip coating.

Author contributions

Conceptualization : M. Hussein , A. Mustafa and M. Abdulkareem; methodology, M. Abdulkareem; software, A. Mustafa; validation, A. Mustafa and M. Abdulkareem; formal analysis, A. Mustafa; investigation, M. Hussein; resources, M. Hussein; data curation, M. Hussein, A. Mustafa and M. Abdulkareem; writing—review and editing, A. Mustafa and M. Abdulkareem; visualization, M. Hussein , A. Mustafa and M. Abdulkareem; supervision:A. Mustafa and M. Abdulkareem; project administration: A. Mustafa and M. Abdulkareem; All authors have read and agreed to the published version of the manuscript.

Funding

This research received no specific grant from any funding agency in the public, commercial, or not-for-profit sectors.

Data availability statement

The data that support the findings of this study are available on request from the corresponding author.

Conflicts of interest

The authors declare that there is no conflict of interest.

References

[1] Q.Y. Wang, Y.B. Wang, J.P. Lin, YF Zheng, Development and properties of Ti-In binary alloys as dental biomaterials, Mater. Sci. Eng. C Mater. Biol. Appl., 33 (2013) 1601-1606. https://doi.org/10.1016/j.msec.2012.12.070

[2] S.S. Bhasin, V. Singh, T. Ahmed, B.P. Singh, Studies on titanium-based dental implant material, In: Kriven WM, Hua-Tay L, editors, 27th Annual Cocoa Beach Conf. Adv. Cem. Compos.,-A: Ceram. Eng. Sci. Proc., 24., (2008)245-54.

[3] Y. Okazaki, S. Rao, Y. Ito, T. Tateishi, Corrosion resistance, mechanical properties, corrosion fatigue strength and cytocompatibility of new Ti alloys without Al and V, Biomaterials, 19 (1998) 1197-215. https://doi.org/10.1016/s0142-9612(97)00235-4

[4] R.B. Heimann, T Anh Vu, M.L. Wayman, Bioceramic coatings: State-of-the-art and recent development trends, Eur. J. Mineral, 9 (1997) 597 - 616. https://doi.org/10.1127/ejm/9/3/0597

[5] M.A. Ur Rehman, F.E. Bastan, Q. Nawaz, W.H. Goldmann, M. Maqbool, S. Virtanen, Electrophoretic deposition of lawsone loaded bioactive glass (BG)/chitosan composite on polyetheretherketone (PEEK)/ BG layers as antibacterial and bioactive coating, J. Biomed. Mater. Res., Part A 2, 106 (2018) 3111–3122. https://doi.org/10.1002/jbm.a.36506

[6] M.A.U. Rehman, M.A. Munawar, D.W. Schubert, Boccaccini AR Electrophoretic deposition of chitosan/gelatin/ bioactive glass composite coatings on 316L stainless steel: A design of experiment study, Surf. Coat. Technol., 358 (2019) 976–986. http://dx.doi.org/10.1016/j.surfcoat.2018.12.013

[7] Y. Wang, C. Wen, P. Hodgson, Y. Li, Biocompatibility of TiO_2 nanotubes with different topographies, J. Biomed. Mater. Res., A, 102 (2013) 743-751. https://doi.org/10.1002/jbm.a.34738

[8] R.B. Heimann, T. Anh Vu, M.L.Wayman , Bioceramic coatings: State-of-the-art and recent development trends, Eur. J. Mineral., 9 (1997) 597–616. https://doi.org/10.1127/ejm/9/3/0597

[9] R. Narayanan, S.K. Seshadri, T.Y. Kwon, K.H. Kim, Calcium phosphate-based coatings on Titanium and its alloys, J. Biomed. Mater. Res., Part B 85 (2008) 279–299. https://doi.org/10.1002/jbm.b.30932

[10] A. Nouri, C. Wen, Introduction to surface coating and modification for metallic biomaterials,: Surf. Coat. Modif. Met. Biomater., (2015) 3–60. https://doi.org/10.1016/B978-1-78242-303-4.00001-6

[11] M. Hekmatfar, S. Moshayedi, S.A. Ghaffari, H.R. Rezaei, F. Golestani-Fard, Fabrication of HAp–8YSZ composite layer on Ti/TiO_2 nanoporous substrate by EPD/MAO method, Mater. Lett., 65 (2011) 3421-3423. https://doi.org/10.1016/j.matlet.2011.07.048

[12] J. Ma, C. Wang, K.W. Peng, Electrophoretic deposition of porous hydroxyapatite scaffold, Biomaterials, 24 (2003) 3505-3510. https://doi.org/10.1016/s0142-9612(03)00203-5

[13] L. Besra, M. Liu, A review on fundamentals and applications of electrophoretic deposition (EPD), Prog. Mater. Sci., 52 (2007) 1 -61. https://doi.org/10.1016/j.pmatsci.2006.07.001

[14] A. Shahriari, H. Aghajani, Electrophoretic Deposition of 3YSZ Coating on AZ91D Alloy Using Al and Ni-P Interlayers, J. Mater. Eng. Perform., 25 (2016) 4369–4382. https://doi.org/10.1007/s11665-016-2253-7

[15] S. Dor, S. Rühle, A. Ofir, M. Adler, L. Grinis, A. Zaban, The influence of suspension composition and deposition mode on the electrophoretic deposition of TiO_2 nanoparticle agglomerates ,Colloids Surf. A Physicochem. Eng. Asp., 342 (2009) 70-75. https://doi.org/10.1016/j.colsurfa.2009.04.009

[16] M. Farrokhi-Rad, S.K. Loghmani, T. Shahrabi, S. Khanmohammadi, Electrophoretic deposition of hydroxyapatite nanostructured coatings with controlled porosity, J. Eur. Ceram. Soc., 34 (2014) 97-106. https://doi.org/10.1016/j.jeurceramsoc.2013.07.022

[17] L. Jia, Z. Lü, X. Huang, Z. Liu, K. Chen, X. Sha, G. Li, W. Su, Editorial Advisory Board, J. Alloys Compd., 424 (2006) 299. https://doi.org/10.1016/S0925-8388(06)01486-1

[18] H. Maleki-Ghaleh, M. Rekabeslami, M.S. Shakeri, M.H. Siadati, M. Javidi, S.H. Talebian, H. Aghajani, Nano-structured yttria-stabilized zirconia coating by electrophoretic deposition, Appl. Surf. Sci., 280 (2013) 666. https://doi.org/10.1016/j.apsusc.2013.04.173

[19] X.Q. Cao,R.Vassen,S. Stöver, Ceramic-materials for thermal barrier coatings, J. Eur. Ceram. Soc., 24 (2004) 1–10. https://doi.org/10.1016/S0955-2219(03)00129-8

[20] W.R. Chen,X.Wu,B.R.Marple,R.S.Lima,P.C.Patnaik, Pre-oxidation and TGO growth behavior of an air-plasma-sprayed thermal barrier coating, Surf.Coat.Technol., 202 (2008) 3787–3796. https://doi.org/10.1016/j.surfcoat.2008.01.021

[21] J. Antony, F.J. Antony, Teaching the Taguchi method to industrial engineers, Work Study, 50 (2001) 141. http://dx.doi.org/10.1108/00438020110391873

[22] R.K. Roy, A Primer, on the Taguchi Method Society of Manufacturing Engineers, The United States of America, 1990.

[23] N. Zaveri, G.D. McEwen, R. Karpagavalli, A. Zhou, Biocorrosion studies of TiO2 nanoparticle-coated Ti–6Al–4V implant in simulated biofluid, J. Nanopart. Res. (2011), doi:10.1007/s11051-009-9699-6.

[24] E. Tabesh, M. Kharaziha, M. Mahmoudi, E. Shahnam, M. Rozbahani, Biological and corrosion evaluation of Laponite®: Poly(caprolactone) nanocomposite coating for biomedical applications, Colloids Surf. A 583 (2019), https://doi.org/ 10.1016/j.colsurfa.2019.123945.

[25] M. Goudarzi, F. Batmanghelich, A. Afshar, A. Dolati, G. Mortazavi, Development of electrophoretically deposited hydroxyapatite coatings on anodized nanotubular TiO_2 structures: corrosion and sintering temperature, Appl. Surf. Sci., 301 (2014) 250–257. https://doi.org/10.1016/j.apsusc.2014.02.055

[26] S. Mahmoodi, L. Sorkhi, M. Farrokhi-Rad, T. Shahrabi, Electrophoretic deposition of hydroxyapatite–chitosan nanocomposite coatings in different alcohols, Surf. Coat. Technol., 216 (2013) 106–114. https://doi.org/10.1016/j.surfcoat.2012.11.032

[27] A.A. Abdeltawab, M.A. Shoeib, S.G. Mohamed, Electrophoretic deposition of hydroxyapatite coatings on Titanium from dimethylformamide suspensions, Surf. Coat. Technol., 206 (2011) 43–50. https://doi.org/10.1016/j.surfcoat.2011.06.034

[28] A. Molaei, M. Yari,M.R. Afshar, Investigation of halloysite nanotube content on electrophoretic deposition (EPD) of chitosan-bioglass-hydroxyapatite-halloysite nanotube nanocomposites films in surface engineering, Appl. Clay Sci.,135 (2017)75-81. https://doi.org/10.1016/j.clay.2016.09.008

[29] M. Farrokhi-Rad, S.K. Loghmani, T. Shahrabi, S. Khan mohammadi, Electrophoretic deposition of hydroxyapatite nanostructured coatings with controlled porosity, J. Eur. Ceram. Soc., 34 (2014) 97–106. https://doi.org/10.1016/J.JEURCERAMSOC.2013.07.022